# ABSOLUTE SOLAR TRANSMITTANCE INTERFEROMETER

**Arthur W. Dybdahl**
**Atmospheric Physics Group**
**Department of Physics and Astronomy**
**University of Denver**
**Denver, Colorado**

## ABSTRACT

The University of Denver's Absolute Solar Transmittance Interferometer (ASTI) has been developed to make high-resolution infrared (IR) radiometric measurements of the incident solar radiance and irradiance at the Earth's surface. It is a research instrument that provides spectral data of high scientific interest in the short-wave infrared (SWIR) band covering 0.97 to 5.13 μm. This band contains about 20 percent of the sun's incident energy, having a significant impact on global as well as regional climate. ASTI spectra are used to provide significant radiometric information describing the SWIR transmittance and absorption properties of the atmosphere. The ASTI research program and instrumentation are described providing information on the research objectives, and for each of its major subassemblies and performance functions. The analytical techniques used to take the instrument data from the basic interferogram to a radiometrically calibrated spectrum is delineated. A high frequency nonlinearity in ASTI's electronics, uncovered during instrument tests and evaluations, is discussed along with the remedial accomplishments displayed in actual solar spectra. Finally, the use of ASTI solar spectra, obtained over a large atmospheric path difference, to measure broadband absorptions in four SWIR regions are related to the possible influence of the $O_2$ continuum in these regions.

## Introduction

The Atmospheric Physics Group of the University of Denver has designed and built ASTI, which is a highly specialized Fourier-transform infrared (FTIR) spectrometric instrument. It is radiometrically calibrated providing absolute measurements of the sun's radiant and irradiant flux at ground level.

The ASTI instrument has been tested, calibrated and its performance evaluated at four locations of differing altitudes and seasons for measuring solar radiance at nearly all times during daylight hours, with emphasis on measurements at and around solar noon. This radiance is measured in the SWIR band from 10,300 to 1,950 wavenumbers (0.97 to 5.13 μm) which contains about 20 percent of the sun's incident energy.

The ASTI Research Program provides accurate calibrated solar spectra obtained at various altitudes from near sea level to over 14,000 feet. ASTI also makes measurements of the SWIR transmittance and scattering properties of varied cloud types for both on-axis and off-axis from solar zenith.

Extensive performance tests, operational tests, and evaluations have been conducted over the past year to assess and improve the instrument's measurement capabilities. A high-frequency nonlinearity was uncovered in and removed from the signal processing electronics of the instrument. Repeatability testing has been conducted to establish ASTI's performance baseline for accurate measurements of solar radiation intensity.

## Background

During the 1980's, significant progress was made in measuring the absolute solar irradiance in the visible and near-IR, both at ground-level and from low-earth orbit, as a part of the Shuttle program. An analytical technique was subsequently developed to effectively extrapolate these measurements to the corresponding exo-atmospheric values as a function of wavenumber and atmospheric mass. This technique is the Langley Extrapolation Technique[1] which employs the modified Langley plots for the extrapolation[2].

In the last decade, the need has strongly arisen for the absolute characterization of the solar SWIR irradiance at the top of the atmosphere and through various atmospheric paths to the earth's surface and, in addition, the SWIR transmittance and scattering properties of all cloud types. These required results will have a major impact on global climate modeling (GCM) work, Earth radiation budget analyses, global warming, and in global and regional climate change assessments.

Characterization of solar SWIR downwelling through the atmosphere along with that of atmospheric aerosol absorption and scattering properties is needed to produce single scattering and scattering phase function albedo measurements for use in atmospheric corrections[3]. Accurate absolute radiometric calibration is required for the atmospheric correction methods being developed by several investigators.

## ASTI, The Research Program

The primary purpose of the ASTI program is to conduct research of high scientific interest and provide the SWIR solar radiance results to the atmospheric physics, meteorology and climatology disciplines.

The primary objectives are: (1) Measure the incident solar flux in the SWIR band from 1,950 to 10,300 wavenumbers ($cm^{-1}$) at ground level, (2) Obtain high resolution SWIR solar spectra, (3) Obtain the spectral values of the solar flux at the top of the earth's sensible atmosphere (Figure 1), the exo-atmospheric flux, and (4) Measure the SWIR scattering properties of various cloud types ranging from high-altitude cirrus to heavy low-altitude cumulus.

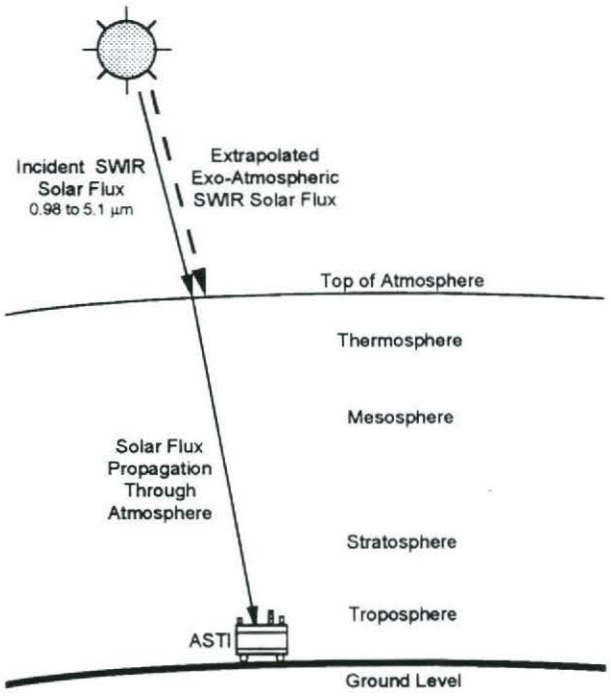


Figure 1 Exo-Atmospheric Extrapolation

ASTI is a one-of-a-kind instrument designed to perform such measurements, which have not been previously conducted either through terrestrial measurements or from space.

The test sites used for ASTI operation are the following along with the respective altitudes: (1) University of Denver, Colorado, 5,400 feet; (2) Near the Summit of Mount Evans, Colorado, 14,100 feet; (3) DOE Southern Great Plains (SGP) Atmospheric Radiation Measurement (ARM) Site, Oklahoma, 1,065 feet; (4) Echo Lake, Colorado, 10,600 feet.

## ASTI, The Instrument

ASTI is a mobile instrument installed on an equipment cart. It is self-contained requiring only external electrical power and liquid $N_2$ for cooling the InSb detector. It is easily transported in a small mini-van.

ASTI is comprised of the following sub-assemblies: (1) Solar constant tracker, (2) Bomem FTIR Spectrometer, (3) Optical shelf, (4) InSb SWIR detector, (5) Power supplies, (6) Calibration Lamp, and (7) PC computer. A functional block diagram of the instrument is shown in Figure 2.

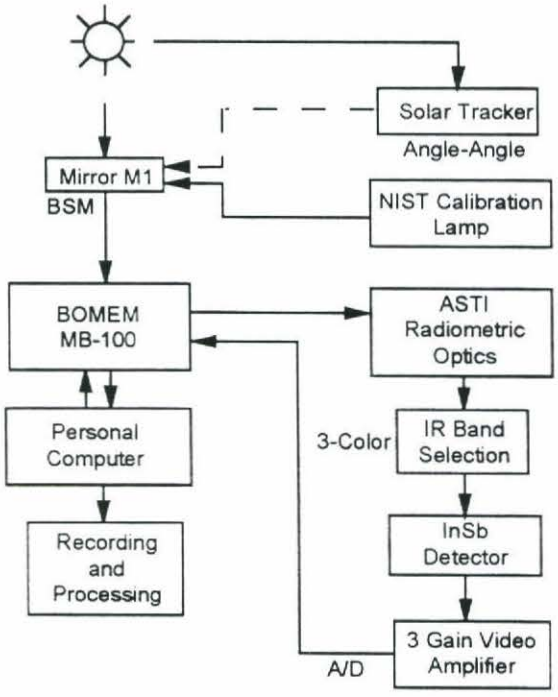


Figure 2 ASTI Functional Block Diagram

## Solar Constant Tracker

This subassembly provides angle-angle tracking of the intense solar disk with an approximate accuracy of 500 μrad. Its purpose is to track the sun from horizon to horizon, ensuring that the solar intensity is always filling the Bomem input aperture. It is able to discriminate solar intensity variations as a function of solar zenith angle with time.

## Bomem FTIR Spectrometer

ASTI employs the interferometric technique[4] for high resolution spectral measurements of the solar intensity at ground level.

The optical path through the instrument is identical for both the input solar radiation and the NIST-calibrated lamp, a major advantage of this design. The input energy is reflected by M1, the solar tracker mirror, and enters the input aperture of the Bomem MB-100 Spectrometer where the interferogram[4] is obtained through a modified continuous-scan Michelson interferometer[5].

The interferometer diverges from the usual Michelson in that it is a double-pendulum design (Figure 3). Instead of a fixed mirror in one position and a movable mirror in the other at a right angle to the fixed mirror, this interferometer uses reflecting corner cubes, both of which are continuously scanned about a common rotation point (top of Figure 3). Both of these mirrors contribute to the effective optical path difference, which produces the interference pattern. The scan rate of the corner cubes is slow, being 0.3436 cm/sec through a distance of 1.0 cm, with a spectral resolution range of 1 to 128 $cm^{-1}$.

The $CaF_2$ self-compensating beam-splitter is optimized for the SWIR band, using the appropriate partially reflective coatings. The beamsplitter is stationary with respect to the moving corner cubes and the instrument chassis.

The zero path difference (ZPD), when the two mirror corner cubes are equidistant from the beamsplitter, is optically detected within the spectrometer using a white light source and maintained by a HeNe laser fringe counter.

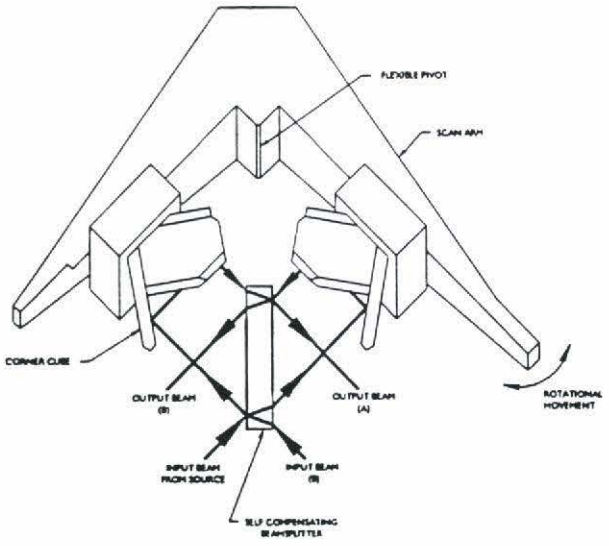


Figure 3 Bomem Michelson Interferometer

## Optical Shelf

The instrument has a long optical path (2.36 m) from the input mirror M1 to the detector, as shown in the optical schematic (Figure 4).

The optical beam then proceeds from the Bomem through the optical shelf where it initially encounters the solar spatial filter F1, which permits the selection of the fraction of the solar disk diameter desired. Filter F2 is a rectangular spatial filter matched to the physical size of the NIST lamp's rectangular filament, ensuring the same optical path as that for solar radiation.

The IR filters F3, F4, F5 are used to select the portions of the required SWIR band used for solar measurements. Their respective band passes are:

Low-band filter - 1,950 to 5,000 $cm^{-1}$,
Medium-band filter - 4,400 to 7,100 $cm^{-1}$,
High-band filter - 6,900 to 10,300 $cm^{-1}$.

The InSb detector converts the SWIR interferogram to an electronic signal, which is sent through the triple-gain amplifier and digitized in the 16 bit Bomem A/D converter. The digital interferogram is then directed to the PC for recording and analysis.

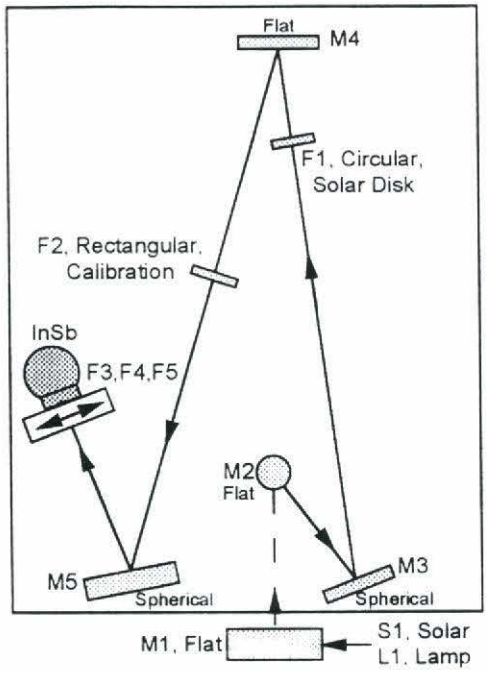


Figure 4 Optical Shelf Schematic Diagram

## Fourier Transform Process

The spectrometer measures an interferogram[4] which is radiation intensity a function of the optical path difference (OPD) of the interferometer's corner cube mirrors from the beamsplitter through the double pendulum interferometer[5]. For a monochromatic incident radiation,

$I(\delta) = (I_o/2)[1 + \cos(2\pi\delta\sigma)]$
$\delta$ = optical path difference
$\sigma = \lambda^{-1}$, wavenumber of input radiation
$\lambda$ = wavelength of radiation

For polychromatic radiation, $I(\delta)$ becomes

$$I(\delta) = (I_o/2)\int_0^\infty S(\sigma)(1 + \cos(2\pi\delta\sigma))d\sigma$$

$$I(\delta) = (I_o/4)\int_{-\infty}^{\infty} S(\sigma)\exp(2\pi\delta\sigma))d\sigma$$

$I_o$ = Incident Radiation Intensity

The desired frequency spectrum $S(\sigma)$ is obtained from the interferogram by a Fourier cosine transformation,

$$S(\sigma) = \int_{-\infty}^{\infty} I(\delta)\exp(-2\pi\delta\sigma)\, d\sigma$$

An interferogram of SWIR solar radiation is given in Figure 5, expanded about ZPD. The corresponding solar spectrum is in Figure 6.

## Apodization of ASTI Spectra

The analytical process of apodization[4-5] is employed to correct the Fourier Transform process for the noisy artifacts in the solar and lamp spectra induced by the abrupt truncation of the scan distance, through the finite scan limits, of the corner cube mirrors. The process involves multiplying the SWIR spectrum by a weighting function which rolls off from the center of the scan pattern. A common form of this function is of the type

$F(D) = (1 + \text{Cos}(\pi D))/2$

D = OPD(from ZPD) / OPD(maximum)

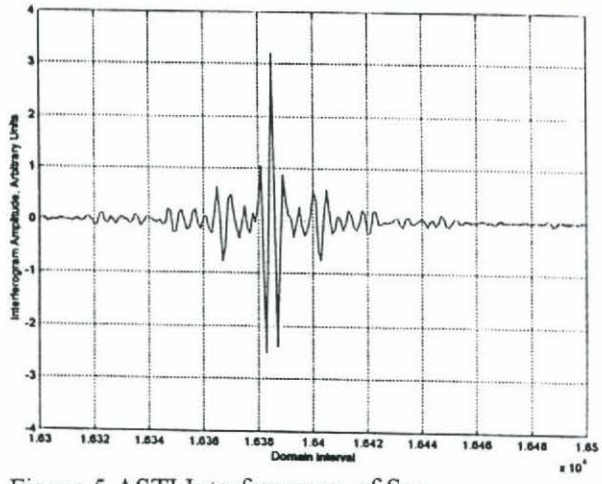


Figure 5 ASTI Interferogram of Sun

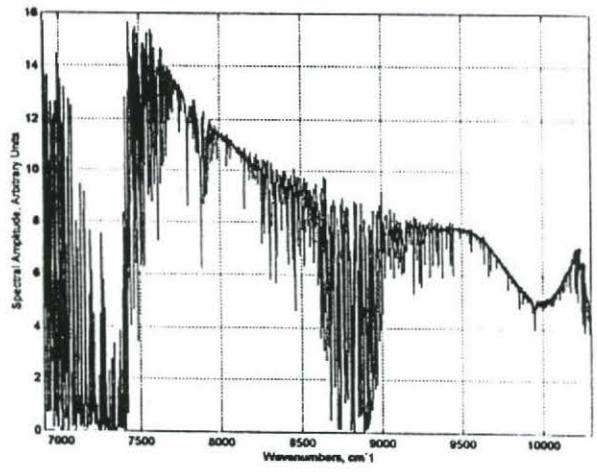


Figure 6 Corresponding Spectrum of Sun

The apodized solar spectrum, an apodized version of Figure 6, is provided in Figure 7. The spikes around 7,500 $cm^{-1}$ are removed.

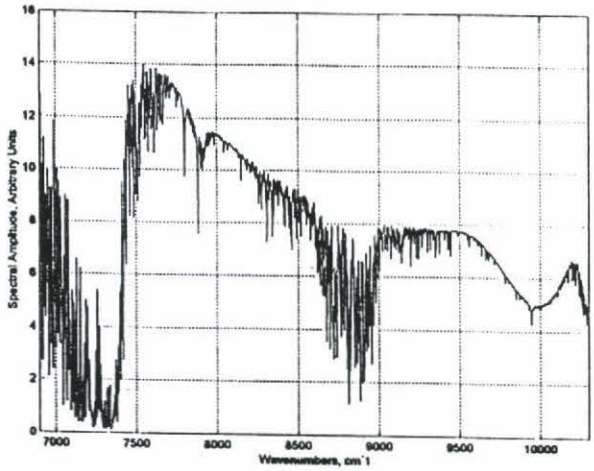


Figure 7 Apodized Spectrum of Sun

## ASTI Calibration

Instrument calibration is accomplished by using a highly-specialized calibration lamp that is itself calibrated and NIST-traceable as a standard of spectral radiance. The lamp has a flat rectangular tungsten ribbon filament measuring 2x8 mm.

The broadband spectral output of the lamp ranges from 1,666 to 40,000 $cm^{-1}$ (6 to 0.25 μm). The SWIR portion of this spectrum used to calibrate ASTI is shown in Figure 8. The units for lamp intensity are Watts/$m^2$ steradian $cm^{-1}$. The instrument measures the spectral radiance from the lamp through the identical optical path that it uses for solar radiance spectra measurement.

With the three lamp spectra and the three corresponding solar spectra, the latter are radiometrically calibrated by the following,

$$I_{Calibrated}(\nu) = [I_{ASTI}(\nu, Sun)/I_{ASTI}(\nu, Lamp)] * S_{manuf}(\nu, Lamp) * G(\nu)$$

$I_{Calibrated}(\nu)$ - Calibrated Solar Spectrum
$I_{ASTI}(\nu, Sun)$ - Raw ASTI Solar Spectrum
$I_{ASTI}(\nu, Lamp)$ - ASTI NIST-Lamp Spectrum

$S_{manuf}(\nu, Lamp)$ - Radiometric Spectrum from Lamp Manufacturer

$G(\nu)$ - ASTI Instrument Gain Factor

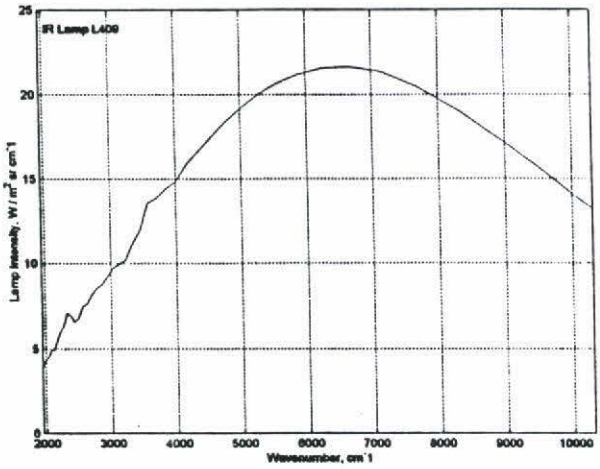


Figure 8 Calibration Lamp Output Spectrum

## Signal Processing Electronics Evaluations

During the extensive performance and operational evaluations of ASTI, a non-linearity as a function of frequency was uncovered in the instrument signal processing electronics. The triple-gain amplifier displayed this effect in the high and medium gain channels, dropping with frequency increase. The noise level increased, Figure 9. The high and medium gain drop off values were 15% and 9%, respectively. The design of the amplifier was modified to correct this problem. The high-gain linearity was measured using solar incident radiance for two input aperture settings, so as to match the respective maximum ZPD values.

Figure 10 shows the flatness of the spectral ratio of these two inputs between the molecular absorption regions. The ratio is clearly unity in these regions throughout the entire SWIR band.

This high frequency nonlinearity was discovered in the analysis of high altitude spectra recorded at 14,100 feet near the summit of Mount Evans. The spectra displayed aberrant amplitude and shape from 7400 to 10,300 $cm^{-1}$, in Figure 11 labeled as 'original.' As a validation, this spectrum was reprocessed using the new lamp calibration spectrum obtained with the modified electronics. The aberrant indications were removed, in Figure 11 labeled as 'reprocessed,' producing proper shape and amplitude.

Figure 12 shows a calibrated SWIR spectrum measured in Denver on April 16, 1997, where all spectra were obtained using the new electronics. The three spectra forming this composite lie within an envelope described by the Planck blackbody equation[6] expressed in the frequency domain. The indicated black body temperature is about 6,250 deg Kelvin.

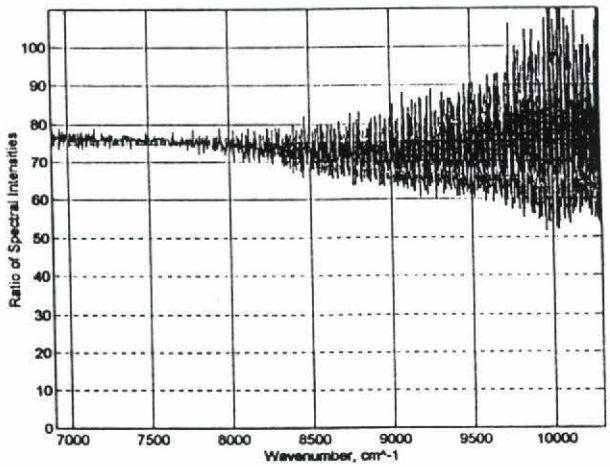


Figure 9 High Frequency Gain Nonlinearity

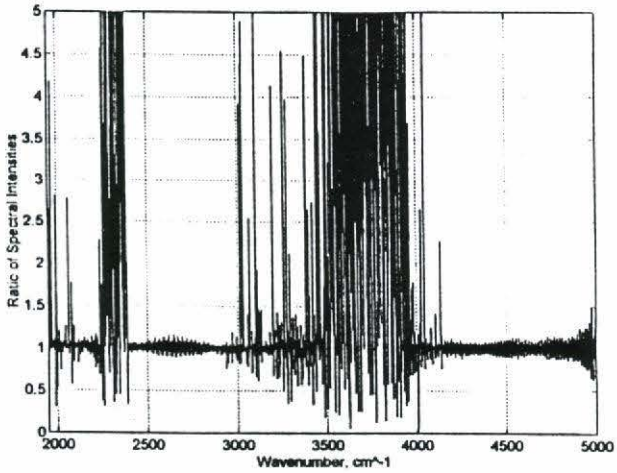


Figure 10 Solar Spectral Ratio - Uniform Gain

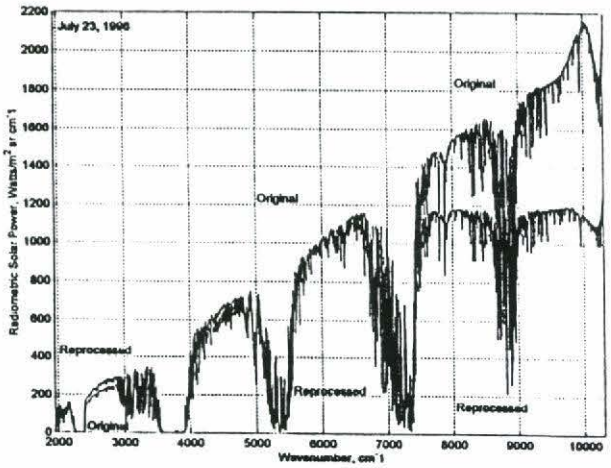


Figure 11 Reprocessed Calibrated Spectrum

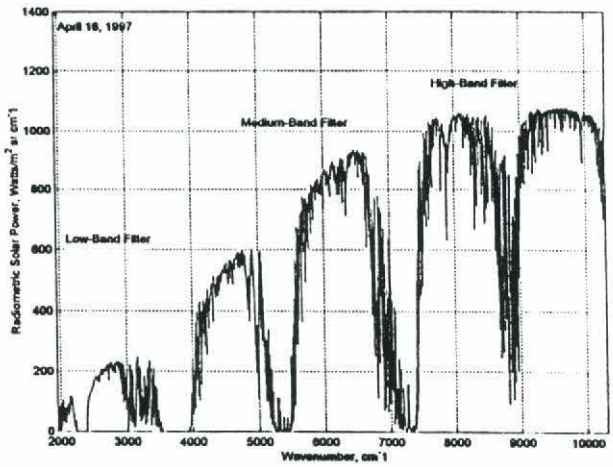


Figure 12 Calibrated SWIR Solar Spectrum

## SWIR Oxygen Continuum

A recent scientific contribution of importance was obtained using ASTI solar spectra[7] in the narrow spectral regions about 1.06 μm (9,366 $cm^{-1}$), 1.27 μm (7,882 $cm^{-1}$) and 1.6 μm (6,326 $cm^{-1}$) as a function of solar zenith.

It is well known that these absorption bands do exhibit both discrete (rotational) line structure and continuous absorption, each of which are of similar intensity.

The modeling of surface SWIR solar irradiance is complex, being reflected in that a comparison of modeling codes used to predict this quantity in GCMs indicated significant discrepancies. The models have been shown to over-predict the intensity of these irradiances when compared with appropriate observations.

The ASTI solar spectra show broad absorption features which appear to be associated with the $O_2$ bands in the above-mentioned narrow regions. These broad absorptions appear to be due to the continuum absorptions of $O_2$. Some of the discrepancy between the calculated and observed SWIR irradiances can be accounted for by this $O_2$ absorption. These indications are quite evident in high resolution spectra (2 $cm^{-1}$ or higher).

The solar spectra obtained at or near solar noon do not emphasize these features. However, the spectra recorded at greater solar zenith angles through longer atmospheric paths do clearly show the broad absorptions.

The two solar spectra in Figure 13 depict the presence of this continuum absorption band around the 9,366 $cm^{-1}$ region [9,200 to 9,600 $cm^{-1}$ (1.087 to 1.042 μm)]. These spectra were obtained at the DOE SGP ARM Site on April 18, 1996. The dotted spectrum was recorded at 13:38 CDT, 32 minutes after solar noon, with an effective optical path through the atmosphere of 1.109 atmospheres. The solid spectrum was recorded at 19:01 CDT, with an optical path of 4.766 atmospheres, a 4.3 times greater path distance than at noon.

The overall extent of this band is from about 9,320 to 9,480 $cm^{-1}$. The broad absorption is barely noticeable in the dotted spectrum, while being quite pronounced in the solid spectrum, recorded 5 hours, 23 minutes later in the day.

This and the other three absorption bands will have to be studied in detail before the results can be treated in any of the atmospheric modeling codes. The high-resolution radiometrically calibrated spectra produced by

ASTI do provide sufficient data to accomplish this task.

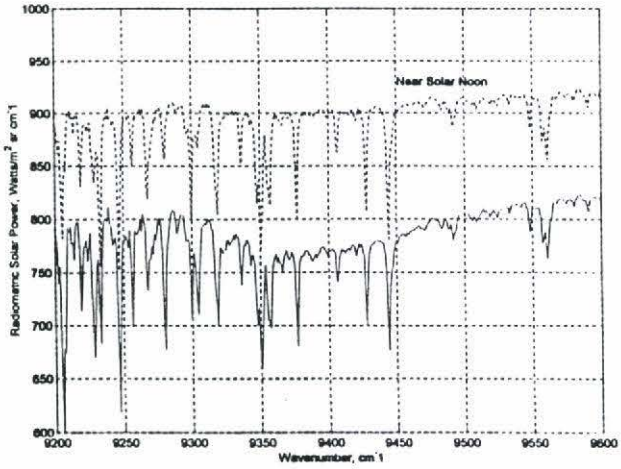


Figure 13 $O_2$ Continuum Band at 1.06 μm

## Acknowledgments

This research project has been supported in part by the Rocky Mountain NASA Space Grant Consortium. Special thanks to Dr. David G. Murcray and Dr. Frank J. Murcray for many helpful discussions, suggestions and overall guidance in the ASTI Program. Thanks to Dr. John Olson, Dr. Joe Landry and Dr. Pierre Fogal for helpful discussions and technical advice.

## Literature Cited

1. **J.A. Reagan, P.A. Pilewskie, I.C. Scott-Flemming, B.M. Herman, A. Ben-David**, "Extrapolation of Earth-Based Solar Irradiance Measurements to Exo-atmospheric Levels for Broad-Band and Selected Absorption-Band Observations," IEEE Transactions of Geoscience and Remote Sensing, Vol. GE-25, 647—653, November 1987
2. **A.S. Moore, L.E. Mauldin III, J.A. Reagan, C.W. Stump, M.G. Fabert**, "Application of the Langley Plot for Calibration Sun Sensors for the Halogen Occulation Experiment (HALOE)," Optical Engineering, Vol. 28, No. 2, 180—187, February 1989.
3. **P.N. Slater, L.D. Mendenhall**, "Executive Summary of the Workshop on Atmospheric Correction of LANDSAT Imagery," August 13, 1993.
4. **P.R. Griffiths, J.A. de Haseth**, "Fourier Transform Infrared Spectroscopy", John Wiley and Sons, 1986, Chapter 1
5. **Bomem, Inc.**, "Michelson Series FT-IR Spectrometer User's Guide", Version 1.50, November 1992
6. **Kuo-Nan Liou**, "An Introduction to Atmospheric Radiation," Academic Press, 1980, Chapter 1
7. **F.J. Murcray, A. Goldman, J.C. Landry, T.M. Stephen**, "$O_2$ Continuum - A Possible Explanation for the Discrepancies Between Measured and Modeled Shortwave Surface Irradiances," Geophysical Research Letters, in press, 1997